Natural damping of time-harmonic waves and its influence on Schwarz methods

Martin Gander[0000−0001−8450−9223] and
Hui Zhang[0000−0001−7245−0674]

1 Introduction

The Helmholtz equation $(\Delta+\omega^2)u = f$ is often used as the prototype time harmonic problem which is difficult to solve by numerical methods, both because high mesh resolutions are required when the wave number ω becomes large and iterative solvers struggle to solve such discretized problems [3]. An idea is to use the shifted Helmholtz equation [7], $(\Delta+\omega^2+i\epsilon)u = f$, also called the Helmholtz equation with damping, and the parameter ϵ can be chosen to make iterative methods succeed, even though a difficult compromise must be chosen between approximation of the Helmholtz equation solution ($\epsilon \leq O(\omega)$ [4]) and easy solvability by iterative methods ($\epsilon \geq O(\omega^2)$ [2]) when using the shifted problem as a preconditioner.

It was shown in [6] that important damping is also coming from the outer boundary conditions applied to the Helmholtz equation, and while it is the closed cavity (all Dirichlet) and the waveguide (Dirichlet along the guide and impedance at the ends) that are the really hard to solve by iterative methods, the free space problem (e.g. impedance all around) becomes as easy to solve as the Laplace problem in the constant coefficient case for Schwarz methods of sweeping type [5] based on optimized Schwarz technology. We show in Fig. 1 a Greens function corresponding to these three cases to illustrate how different the solution looks like.

We are interested here in studying if natural damping mechanisms coming from the physical properties of the wave phenomenon one wants to study can make the damped Helmholtz problem easy to solve by such Schwarz methods. To do so, we go back to the underlying phyiscal wave equation from which the Helmholtz equation

Martin Gander
Department of Mathematics, University of Geneva, Rue du Général Dufour, 1211 Genève 4, Switzerland, e-mail: martin.gander@unige.ch

Hui Zhang (corresponding)
Department of Applied Mathematics, Xi'an Jiaotong-Liverpool University, 111 Ren'ai Road, 215123 Suzhou, China, e-mail: hui.zhang@xjtlu.edu.cn

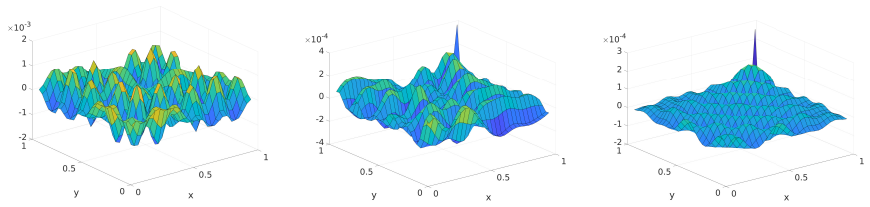

Fig. 1 Greens function for 3 Helmholtz problems. Left: closed cavity; middle: wave guide; right: free space, where optimized Schwarz solvers are as effective as for Laplace problems [6].

arises, namely the second order wave equation, $u_{tt} = \Delta u + f$. There are two main damping mechanisms that arise in nature for damping solutions of the second order wave equation, first order and viscoelastic damping,

$$u_{tt} + ru_t = \Delta u + \gamma \partial_t \Delta u + f, \tag{1}$$

where r is the first order damping strength, and γ is the viscoelastic damping strength. These terms are present in all physical phenomena in nature, the second order wave equation is a simplifying model, and waves never remain forever, there is always damping. If the source $f(x,t)$ and the solution $u(x,t)$ have the time-harmonic form $\hat{f}(x)e^{i\omega t}$ and $\hat{u}(x)e^{i\omega t}$, then we find $(\omega^2 - i\omega r)\hat{u} + (1 + i\omega\gamma)\Delta\hat{u} = -\hat{f}$, which we write it in the normalized form (omitting the hats) to obtain the new Helmholtz equation that includes natural damping,

$$\Delta u - \eta u = -f/(1 + \gamma i\omega), \quad \eta := -\omega^2(1 - ri\omega^{-1})(1 + \gamma i\omega)^{-1}. \tag{2}$$

We show in Figure 2 the influence of first order and viscoelastic damping on the Greens functions from Figure 1. We see that both types of damping make the Greens function look like the easy to solve case in Figure 1 on the right, all difficulties from the closed cavity and wave guide configurations seem to have disappeared. It is therefore of interest to investigate the performance of Schwarz methods in these naturally damped configurations.

We analyze here the parallel Schwarz method applied to (2) on the domain $\Omega := (0,1)^2$ with impedance transmission conditions at subdomain interfaces of the form $\partial_{\mathbf{n}} u + \sqrt{\eta} u$, where $\mathbf{n}$ is the unit normal. We decompose the domain along the x direction into overlapping subdomains of the same width $H + L$ with L the overlap width shared by two neighbors. We apply Fourier series in y, then calculate numerically the spectral radius of the iteration matrix of the interface values $\partial_{\mathbf{n}} u + \sqrt{\eta} u$, which we call convergence factor ρ, and present results both for the waveguide and the closed cavity problems.

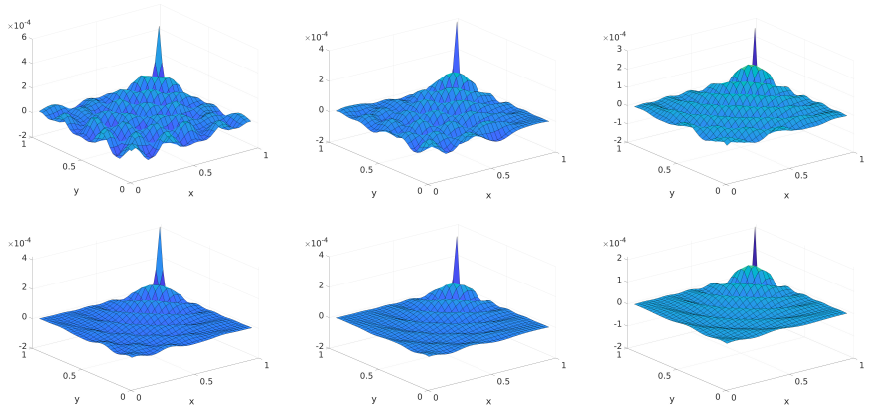

Fig. 2 Greens functions with first order damping $r = 1$ (top) and viscoelastic damping $\gamma = 0.003$ (bottom).

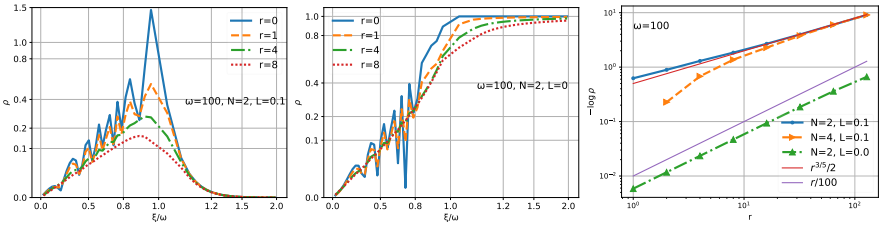

Fig. 3 Convergence factor dependence on r for the waveguide with the operator $\Delta + \omega^2 - \mathrm{i}\omega r$

2 Waveguide problem

In the waveguide problem, $\partial_{\mathbf{n}} u + \sqrt{\eta} u = 0$ at $x \in \{0, 1\}$, and $u = 0$ on the other sides, and we consider first order damping ($r > 0$, $\gamma = 0$) and viscoelastic damping ($r = 0$, $\gamma > 0$) separately. We visualize the convergence factor ρ in the Fourier domain with ξ the Fourier frequency for y.

2.1 Helmholtz operator $\Delta + \omega^2 - \mathrm{i}\omega r$ in the waveguide

We first measure how the convergence factor scales with the damping coefficient r; see Fig. 3. We see that the damping helps not only convergence of the propagating modes ($\xi/\omega < 1$) but also the evanescent modes ($\xi/\omega > 1$), and that the benefit is more notable for the nonoverlapping method ($L = 0$) and its evanescent modes. On the right, we see that the convergence factor goes to zero exponentially when $r \to \infty$, indicating very fast convergence.

Next, we study the scalings with respect to the wavenumber ω, number of subdomains N and the overlap width L. On many subdomains, the overlap width L has

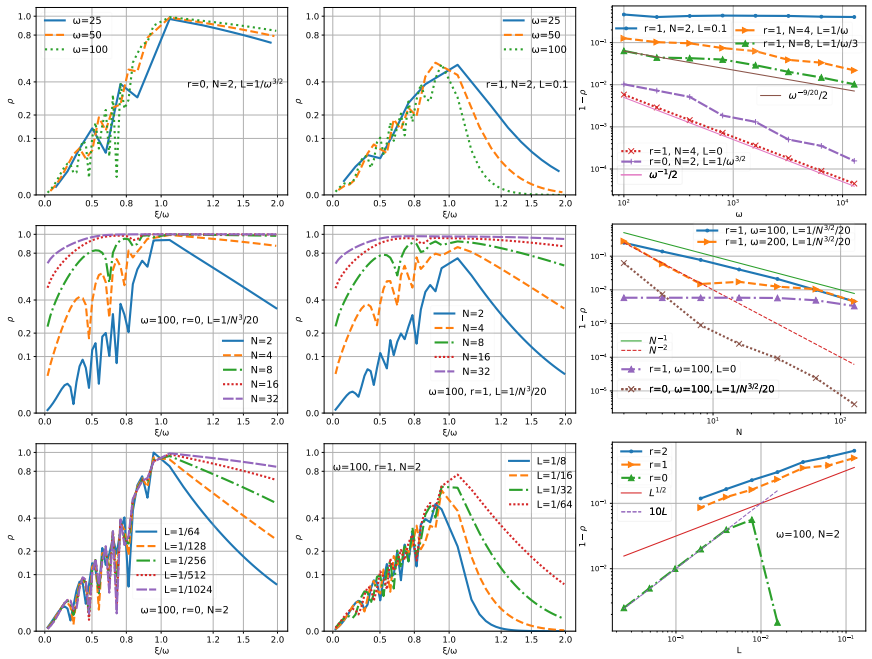

Fig. 4 Convergence factor dependence on ω (top), number of subdomains N (middle) and overlap L (bottom) for the waveguide with the operator $\Delta + \omega^2 - \mathrm{i}\omega r$

to be sufficiently small with respect to the wavenumber ω and the number of subdomains N to ensure convergence without physical damping [6]. Actually, for each given ω and N, there would be an optimal overlap width, but we will not seek the optimal L in this note and just use an ad hoc choice. Fig. 4 show that the waveguide problem with first order damping has similar scalings to the free space problem without damping in [6], while the waveguide problem without damping has much different scalings and is more difficult to solve by the Schwarz method. In particular, the top row in Fig. 4 shows that the Schwarz method on two fixed subdomains is robust in the wavenumber with damping, but not on many subdomains or without damping.

2.2 Helmholtz operator $(1 + \mathrm{i}\omega\gamma)\Delta + \omega^2$ in the waveguide

As we mentioned, the Helmholtz equation $(1+\mathrm{i}\omega\gamma)\Delta u+\omega^2 u = f$ may be normalized to $\Delta u + u\omega^2/(1 + \mathrm{i}\omega\gamma) = f/(1 + \mathrm{i}\omega\gamma)$. The 0th order coefficient is then

$$\omega^2/(1 + \mathrm{i}\omega\gamma) = \frac{\omega^2}{1 + \omega^2\gamma^2}(1 - \mathrm{i}\omega\gamma) \approx \begin{cases} \omega^2 - \mathrm{i}\omega^3\gamma & \text{if } \omega\gamma \ll 1 \\ c\omega^2(1 - \mathrm{i}) & \text{if } \omega\gamma \approx 1 \text{ and } \frac{1}{1+\omega^2\gamma^2} = c \\ \gamma^{-2} - \mathrm{i}\omega\gamma^{-1} & \text{if } \omega\gamma \gg 1 \end{cases},$$

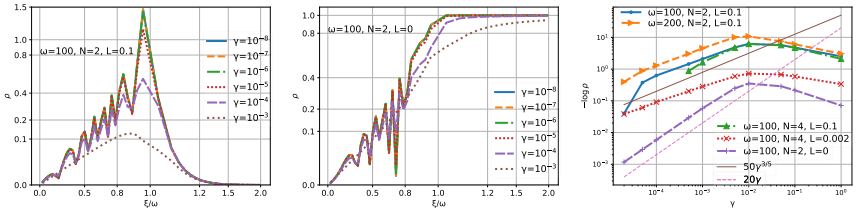

Fig. 5 Convergence factor dependence on γ for the waveguide with the operator $(1+\mathrm{i}\omega\gamma)\Delta+\omega^2$

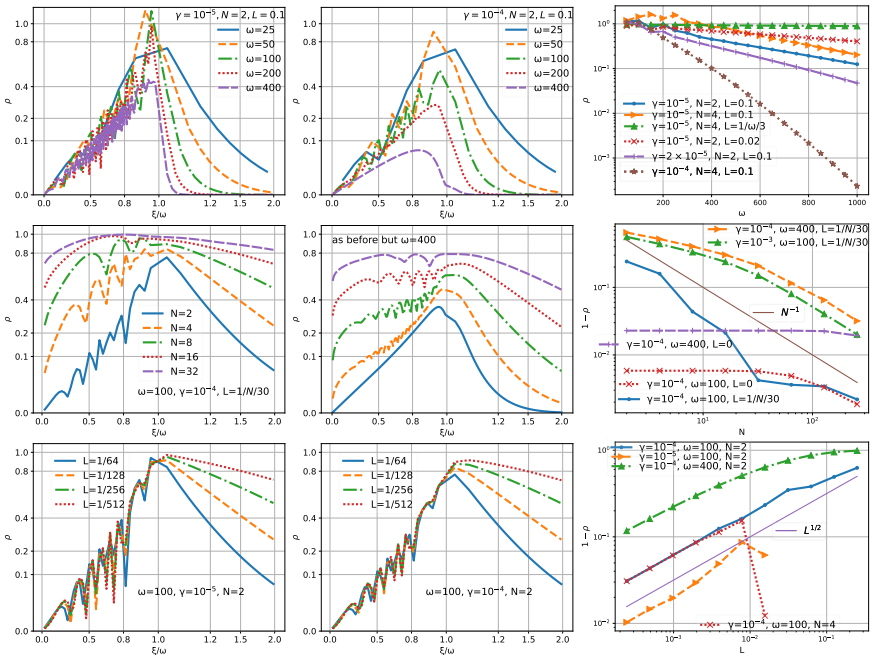

Fig. 6 Convergence factor dependence on ω (top), number of subdomains N (middle) and overlap L (bottom) for the waveguide with the operator $(1+\mathrm{i}\omega\gamma)\Delta+\omega^2$

and, with no approximation, the ratio of the imaginary part to the real part is $-\omega\gamma$. Fig. 5 shows the scaling of the convergence factor with γ. Note that $\gamma = 0$ here is the same as the no damping case $r = 0$ in Sect. 2.1, so $\gamma = 0$ is not shown here. But compared to Fig. 3 with $\omega = 100$ the small dampings $\gamma = 10^{-8}, 10^{-7}, 10^{-6}$ almost coincide with the no damping case, while $\gamma = 10^{-4}$ roughly mimics $r = \omega^2\gamma = 1$.

However, this does not imply that the viscoelastic damping in $(1+\mathrm{i}\omega\gamma)\Delta+\omega^2$ is the same as the first order damping in $\Delta+\omega^2-\mathrm{i}\omega r$: the latter has the imaginary/real ratio $-r/\omega$. So we can expect the two types of damping to differ significantly with large ω. This is clearly visible in the first line of Fig. 6 which is drastically different from the first line in Fig. 4. The scaling with number of subdomains is shown in Fig. 6 (middle). For moderate wavenumber, sufficiently small overlap is still required for

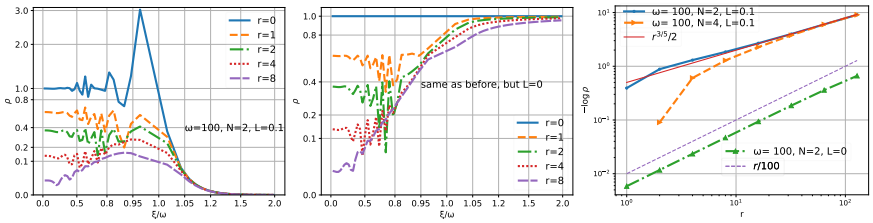

Fig. 7 Convergence factor dependence on r for the cavity with the operator $\Delta + \omega^2 - \mathrm{i}\omega r$

convergence on many subdomains. There is an optimal overlap width L for given ω, γ and N, which is not investigated here. But with the ad hoc choice of $L = O(N^{-1})$ we get the typical scaling $\rho = 1 - O(N^{-1})$ for one-level parallel Schwarz methods applied to Laplace problems.

In the bottom row of Fig. 6, we show the dependence on the overlap width L. The scaling with small overlap is the same as Fig. 4 (bottom), also the same requirement of smaller overlap for more subdomains. But here larger wavenumbers can lead to faster convergence and allow using larger overlap.

3 Cavity Problem

In the closed cavity problem, $u = 0$ on all the boundary. For wellposedness of the problem without damping, we assume the squared wavenumber ω^2 is not an eigenvalue of the negative Laplace operator.

3.1 Helmholtz operator $\Delta + \omega^2 - \mathrm{i}\omega r$ in the cavity

The influence of the first order damping coefficient r is shown in Fig. 7. Compared to Fig. 3 for the waveguide problem, here for the cavity problem the low space frequency has a larger convergence factor. But this difference quickly diminishes as r increases, and the scaling for r large remains the same, so even the very hard closed cavity problem becomes easy with first order damping.

We show in Fig. 8 the corresponding dependence on the other parameters. We see that without first order damping the Schwarz method for the closed cavity problem can not converge at all; see Fig. 8 (top left). With first order damping, convergence is robust in ω for two subdomains as in the wave guide case, and deteriorates similarly for more subdomains. From the green line ($r = 1$, $N = 8$, $L = 1/\omega/3$), we can see that, as ω gradually increases, the convergence here is first slower than, and then close to, the convergence in the wave guide case.

3.2 Helmholtz operator $(1 + \mathrm{i}\omega\gamma)\Delta + \omega^2$ in the cavity

We finally show the influence of the viscous damping coefficient γ Fig. 9. We see that similarly to the first order damping, the behavior of the very hard closed cavity

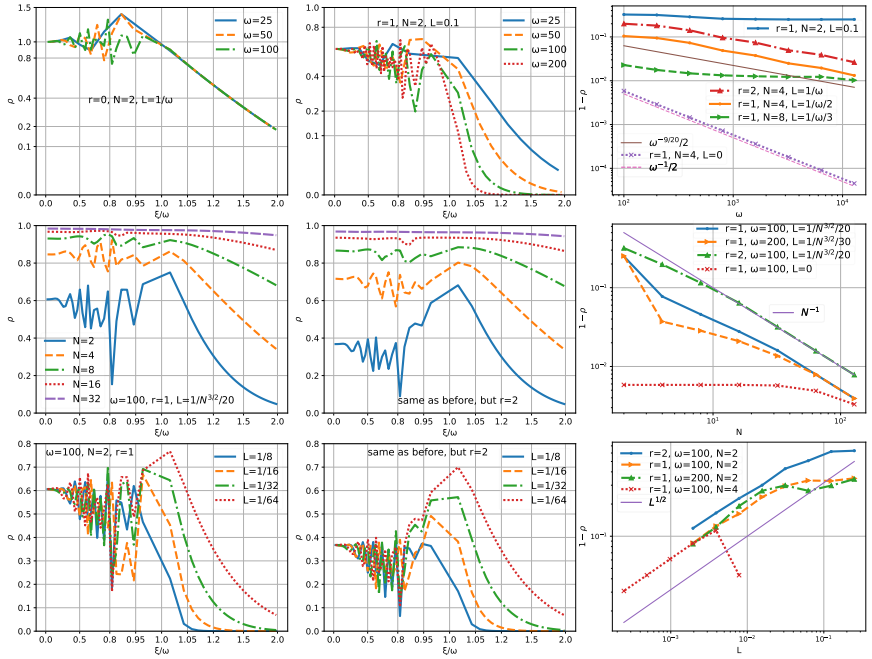

Fig. 8 Convergence factor dependence on ω (top), number of subdomains N (middle) and overlap L (bottom) for the cavity with the operator $\Delta + \omega^2 - \mathrm{i}\omega r$

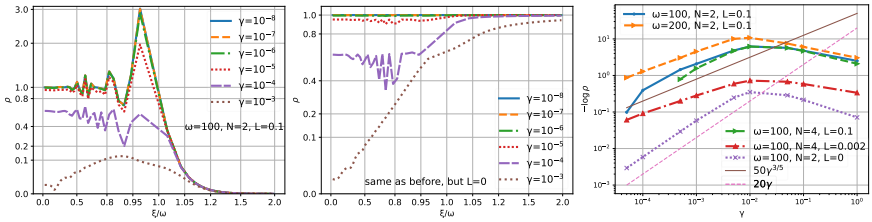

Fig. 9 Convergence factor dependence on γ for the cavity with the operator $(1 + \mathrm{i}\omega\gamma)\Delta + \omega^2$

case becomes comparable to the wave guide case, especially at $\gamma = 10^{-3}$, though, at smaller γ, the convergence at the space low frequency is slower than that in the wave guide. The corresponding dependence on the other parameters is shown in Fig. 10.

4 Conclusions

The damping $\omega^2 \mapsto \omega^2 + \mathrm{i}\omega$ or $\Delta \mapsto (1 + \mathrm{i}\omega 10^{-4})\Delta$ helps the optimized Schwarz method for the wave guide and cavity problems scale similarly to that for the free space problem. The scalability w. r. t. number of subdomains N is not seen in this paper, but only seemingly for $N \leq 100$ with no overlap. A limiting formula for $N \to \infty$ and the scalability for large N with sufficient damping can be found in [1].

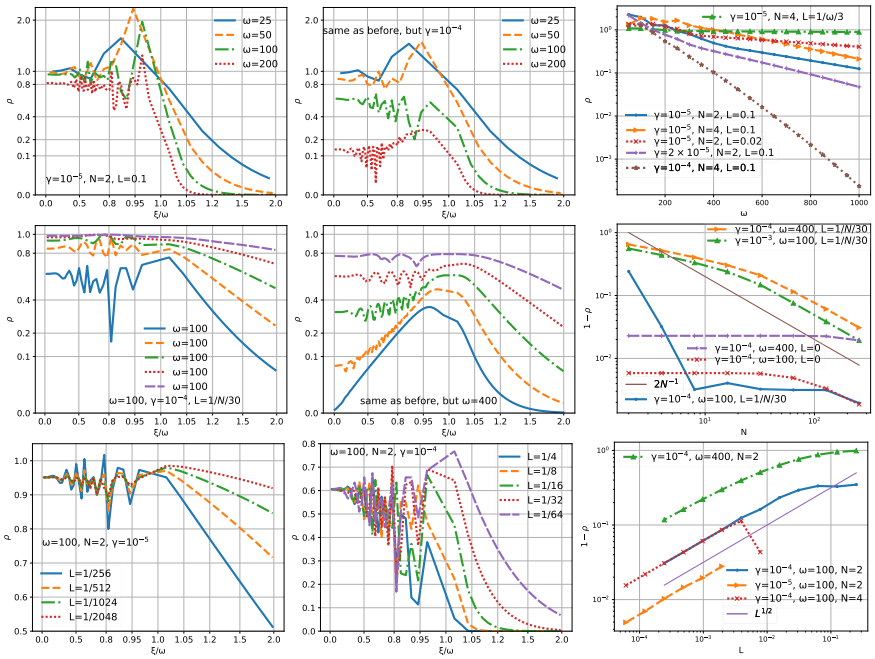

Fig. 10 Convergence factor dependence on ω (top), number of subdomains N (middle) and overlap L (bottom) for the cavity with the operator $(1+\mathrm{i}\omega\gamma)\Delta+\omega^2$

References

1. Bootland, N., Dolean, V., Kyriakis, A., Pestana, J.: Analysis of parallel Schwarz algorithms for time-harmonic problems using block Toeplitz matrices. Electronic Transactions on Numerical Analysis pp. 112–141 (2022)
2. Cocquet, P.H., Gander, M.J.: How large a shift is needed in the shifted Helmholtz preconditioner for its effective inversion by multigrid? SIAM Journal on Scientific Computing **39**(2), A438–A478 (2017)
3. Ernst, O.G., Gander, M.J.: Why it is difficult to solve Helmholtz problems with classical iterative methods. Numerical analysis of multiscale problems pp. 325–363 (2011)
4. Gander, M.J., Graham, I.G., Spence, E.A.: Applying GMRES to the Helmholtz equation with shifted Laplacian preconditioning: what is the largest shift for which wavenumber-independent convergence is guaranteed? Numerische Mathematik **131**(3), 567–614 (2015)
5. Gander, M.J., Zhang, H.: A class of iterative solvers for the Helmholtz equation: Factorizations, sweeping preconditioners, source transfer, single layer potentials, polarized traces, and optimized Schwarz methods. Siam Review **61**(1), 3–76 (2019)
6. Gander, M.J., Zhang, H.: Schwarz methods by domain truncation. Acta Numerica **31**, 1–134 (2022)
7. Van Gijzen, M.B., Erlangga, Y.A., Vuik, C.: Spectral analysis of the discrete Helmholtz operator preconditioned with a shifted laplacian. SIAM Journal on Scientific Computing **29**(5), 1942–1958 (2007)